Energy bands, Compton profile, and optical conductivity of vanadium*

D. G. Laurent, C. S. Wang,† and J. Callaway
Department of Physics and Astronomy, Louisiana State University, Baton Rouge, Louisiana 70803
(Received 6 June 1977)

A self-consistent calculation of energy bands in vanadium has been performed using the linear-combination-of-atomic-orbitals method. The basis contained 13 s-type, ten p-type, five d-type, and one f-type Gaussian orbitals. A local exchange potential of the Kohn-Sham form was included. Results are presented for the band structure, density of states, Compton profile, and optical conductivity.

I. INTRODUCTION

The band structure of vanadium has been the subject of several investigations.[1-7] The present calculation was undertaken primarily in order to compute accurate Compton profiles. Such a computation requires us to generate energy bands, and we have explored the resulting Fermi surface. In addition, we have calculated the optical conductivity including $\vec{k}$-dependent matrix elements.

Our self-consistent calculation employs the linear-combination-of-atomic-orbitals (LCAO) method with a basis consisting of independent Gaussian functions. It parallels, in computational aspects, a recently reported calculation of energy bands in nickel,[8] to which the reader is referred for additional details concerning methods. In the present work, we have employed solely the Kohn-Sham-Gaspar local exchange potential.[9] No muffin-tin approximation is involved in these calculations.

The Bloch wave functions were expanded in a set of independent Gaussian orbitals, including thirteen of s symmetry, ten p, five d, and one f. The Hamiltonian and overlap matrices are of dimension 75×75. The exponents of the s, p, and d orbitals were those used by Wachters in a self-consistent calculation for the free vanadium atom[10] except that the s and p orbitals of longest range were discarded. The f orbital was chosen to have the exponent 0.9. The lattice constant was taken to be 5.7448 a.u.

The charge density for the first cycle of the iterative procedure was that of a superposition of neutral-vanadium-atom (configuration d^4s^1) charge densities. This was obtained using Wachters' wave functions; although these were calculated for a configuration d^3s^2. The iterations leading to self-consistency were continued until the change in the leading Fourier coefficient of potential was 0.0001 Ry or less. The charge density was sampled at 140 points in $\frac{1}{48}$ of the Brillouin zone. After the completion of the self-consistent cycle, energy levels and wave functions were evaluated at 506 points in the irreducible wedge. The density of states was evaluated by the linear analytic tetrahedron method.[11-14]

II. BAND STRUCTURE AND DENSITY OF STATES

Our calculated energy bands are shown along certain symmetry directions in Fig. 1. Selected energy values at symmetry points are given in

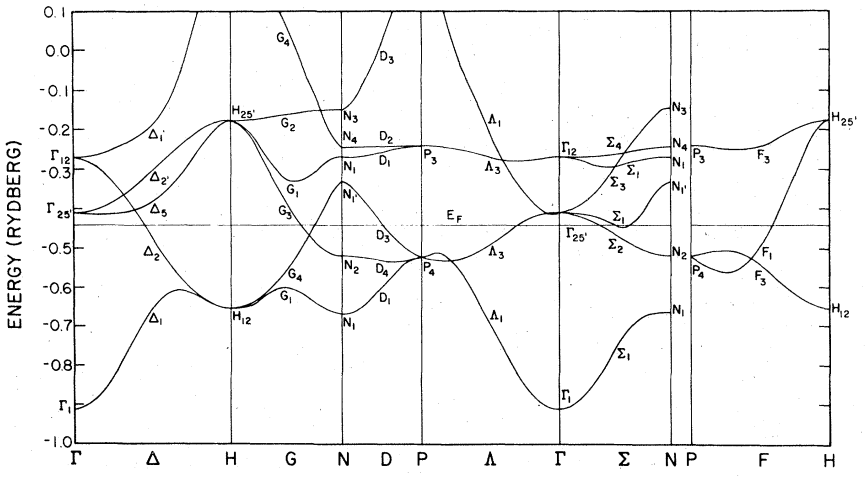

FIG. 1. Energy bands in vanadium along some lines of high symmetry.

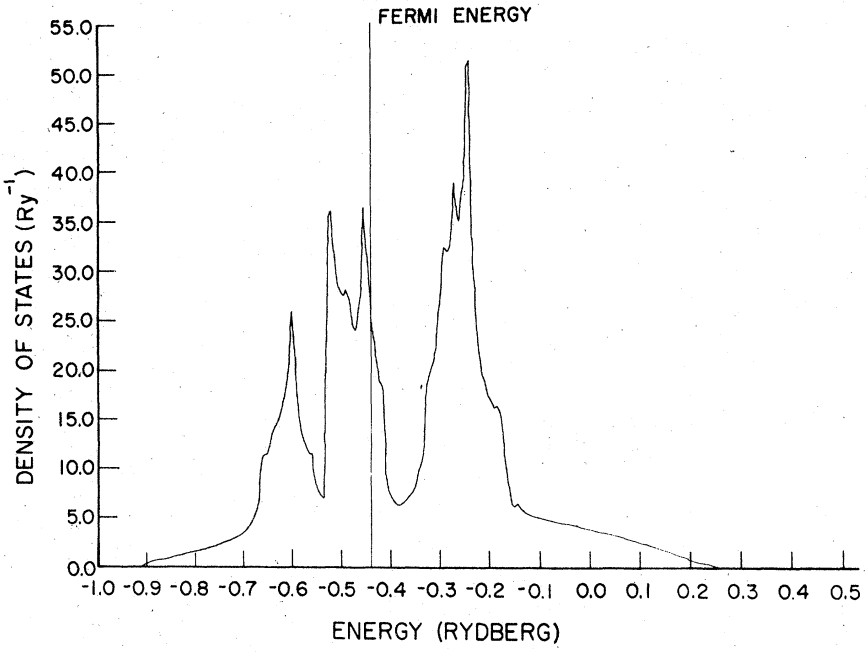

FIG. 2. Density of states.

Table I. There is a reasonable degree of agreement between the characteristic energy-level separation ($\Gamma_{25'}$-Γ_1, $H_{25'}$-H_{12}, etc.) and those listed by Wakoh and Yamashita[5] for the same potential. Our values for these separations agree within 0.01 Ry except for the case Γ_{12}-$\Gamma_{25'}$, where our energy difference is larger than theirs by 0.015 Ry. The agreement with the calculation of Papaconstantopoulas *et al.*[4] is not so good. For example, the values for $E(H_{25'}) - E(H_{12})$ differ by 0.06 Ry.

Some overall measures of our band structure are the following. The width of the occupied portion of the d band, measured by $E_F - E(N_1)$ is 3.1 eV, while the total d-band width including unoccupied states (estimated as N_3-N_1) is 7.0 eV. The total occupied bandwidth, including s states below the d band $[E_F - E(\Gamma_1)]$ is 6.4 eV. The occupied band widths seem to be in reasonable accord with the experiment.[15,16]

TABLE I. Selected energy levels of electrons in vanadium. Energies are in rydbergs.

Γ_1	−0.9098	N_1	−0.6649
$\Gamma_{25'}$	−0.4098	N_2	−0.5176
Γ_{12}	−0.2688	N_1'	−0.3319
		N_1	−0.2687
H_{12}	−0.6510	N_4	−0.2443
$H_{25'}$	−0.1753	N_3	−0.1476
P_4	−0.5206		
P_3	−0.2401		

$E_F = -0.4397$

The density of states is shown in Fig. 2. We find a value of the density of states at the Fermi energy $N(E_F) = 25.03$ Ry^{-1}. This is considerably smaller than that determined from specific-heat measurements, $N(E_F) = 57.26$ Ry^{-1}.[17] The difference between the calculated value and experiment amounts to a factor of 2.29, which is much larger than conventionally attributed to phonon renormalization (1.6),[18] and substantially larger than found in our previous calculations for nickel and iron.[19] Boyer, Papaconstantopoulos, and Klein[7] obtained $N(E_F) = 20.146$ Ry^{-1} for the Kohn-Sham (KS) potential and $N(E_F) = 25.76$ Ry^{-1} from an $X\alpha$ calculation with $\alpha = 0.715\,56$. Evidently the substantial disagreement with experiment is not simply an artifact of the present computation. Perhaps further studies of electron-phonon and electron-electron interaction effects on the density of states are required.

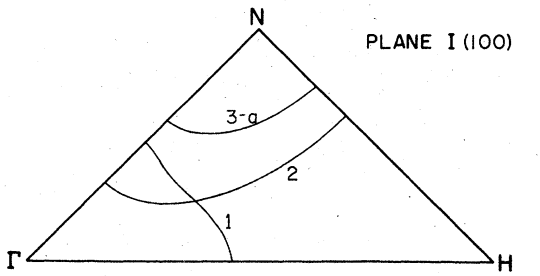

FIG. 3. Cross sections of the vanadium Fermi surface in a (100) plane. The surfaces are identified as 1, 2, 3, as described in the text. The designation α, in reference to surface 3, refers to the orbit I-α shown in Fig. 5.

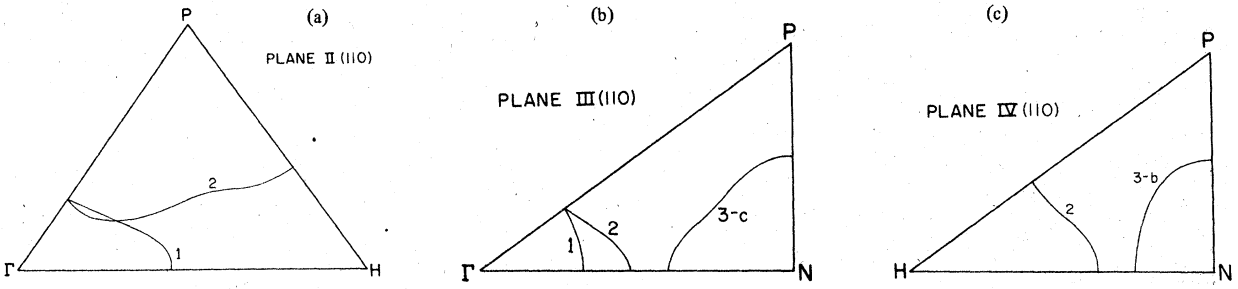

FIG. 4. Cross sections in portions of a (110) plane. (a) (plane II), Γ-*H*-*P*; (b) (plane III), Γ-*N*-*P*; (c) (plane IV), *H*-*N*-*P*. The surfaces are as described in the text. Curves 3-*c* and 3-*b* in planes III and IV refer to orbits shown in Fig. 5.

III. FERMI SURFACE

We have studied the Fermi surface resulting from these calculations. Cross sections are shown in Figs. 3 and 4(a)–4(c). It is useful to distinguish three sheets, two of which are connected.

(i) Hole surface around Γ. This is formed from states in the second band. It is closed, except for points of contact with surface 2 in (110) and (111) planes. It has not been observed experimentally.

(ii) Jungle gym. This surface consists of third band hole tubes running along [100] directions. It connects with surface 1 in (100) and (110) planes, forming a complex, multiply connected structure. An orbit around a tube has been observed.[20]

(iii) Electron surfaces, around *N*. There are six such surfaces, which resemble ellipsoids but are flatter, as well as slightly fluted. They have been well investigated experimentally.[20,21] Several different cross sections have been observed. They are identified as I-*a*, etc., and are most easily visualized with the aid of Fig. 5.

Points on the Fermi surface were located by interpolation. Our values for cross-sectional areas are presented and compared with the results of magnetothermal oscillation[20] and de Haas-van Alphen effect[21] measurements in Table II. The calculated areas are (15–20)% larger than the experimental values, except in the case of the jungle gym, where our cross section is smaller. Similar discrepancies (not, however, specified quantitatively) were noted by Wakoh and Yamashita.[16] Areas of these cross sections have also been calculated by Boyer *et al.*[7] using a Slater-Koster fit to the band structure. They are included in Table II. The areas reported by these authors are consistently smaller than those we have obtained (except for surface II). Wakoh and Yamashita have also apparently obtained cross sections larger than experimental for the KS potential (their cross sections are only shown graphically, no numbers are given).

The discrepancy between the results of the present work and that of Ref. 7 probably results more from differences in the band structure than from the method of locating the Fermi surface. We do not know why these differences (also mentioned in Sec. II) exist: possibly the muffin-tin approximation of the usual APW method plays some role; or possibly there are some limitations on the degree of self-consistency obtained by those authors.

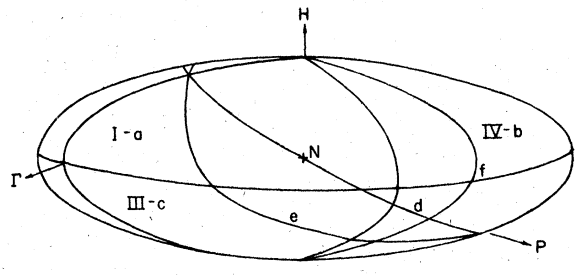

FIG. 5. Orbits around the *N*-centered ellipsoids.

IV. X-RAY FORM FACTOR AND COMPTON PROFILE

The calculated x-ray form factor is listed in Table III. We have been unable to locate much experimental data. The (1, 1, 0) and (2, 0, 0) form factors have been determined by Terasaki *et al.*[22] Our results agree with these within the quoted experimental error. Measurements of the form factor ratios for the (330) and (411) reflections have been reported by Weiss and DeMarco[23] and Diana and Mazzone.[24] The results (1.024 and 1.0085, respectively,) are much larger than our values.

We have calculated the Compton profile of vanadium using the wave functions generated in the band calculation. A grid of 506 points in the irreducible wedge of the Brillouin zone was used. Our procedures have been described elsewhere.[25] A similar calculation has been reported by Wakoh, Kubo, and Yamashita,[26] using wave functions obtained from an APW band calculation.

TABLE II. Areas of cross sections of the vanadium Fermi surface. The surface numbering (2,3) refers to the text. The section numbers refer to Fig. 5. The cross section of surface 2 is in a plane perpendicular to a (100) axis, but not passing through Γ (and is not shown in the figures).

Surface	Section	Calculated area (nm^{-2}) Present	Ref. 7	Observed area (nm^{-2}) Ref. 20	Ref. 21
		(100) plane			
2		24	42	32	
3	*d*	67	54	57.6	57.5
	I-*a*	60	40	50.5	50.2
		(110) plane			
3	*e*	58	45	50.4	50.7
	IV-*b*	60	53	53.1	53.2
	III-*c*	72	54	64.1	64.1
		(111) plane			
3	*f*	55	46	47.9	

The calculated Compton profile includes only band electrons ($4s+3d$). The contribution from the spherically symmetric core can be calculated satisfactorily from atomic Hartree-Fock wave functions. These values are already in the literature.[27]

Our numerical values for $J_{\hat{k}}(q)$ (see Ref. 25 for definitions) in the [100], [110], and [111] directions, together with the angular average are given in Table IV. In Fig. 6, the average profile is compared with the results of Phillips,[27] from which the core contribution has been subtracted. The agreement is quite satisfactory. Other measurements have been reported by Manninen and Paakkari[28] which are in good agreement with those of Phillips.

The present results agree rather well with the calculations of Wakoh, Kubo, and Yamashita for small values of q ($q \leq 0.5$). The maximum disagreement is 3% in a single case, and more typically the results agree within (1–2)%. However for large q, our values of J become consistently larger than theirs, for all directions. At $q=2.5$ (the largest value they report) the discrepancy approaches 50% for the [110] direction. We can not give a definite reason for this disagreement, but are inclined to suspect that their APW wave functions may not have converged adequately.

Figures 7(a)–7(b) show our calculated results for the anisotropy of the profile. Measurements have been reported by Terasaki *et al.*[29]; however, the results are given graphically only and in figures too small to permit extraction of numbers. However, there appears to be some degree of agreement.

TABLE III. X-ray form factor of vanadium.

Wave vector $a\vec{K}/2\pi$	Present calculation	Experimental Ref. 22
(1,1,0)	15.752	15.90 ±0.18
(2,0,0)	13.113	13.22 ±0.17
(2,1,1)	11.434	
(2,2,0)	10.229	
(3,1,0)	9.323	
(2,2,2)	8.727	
(3,2,1)	8.216	
(4,0,0)	7.778	
(3,3,0)	7.516	
(4,1,1)	7.487	
(3,3,0)/(4,1,1)	1.0039	
(4,2,0)	7.239	
(3,3,2)	7.046	
(4,2,2)	6.842	
(4,3,1)	6.671	
(5,1,0)	6.636	

V. OPTICAL CONDUCTIVITY

We have calculated the interband optical conductivity by integration over the Brillouin zone. The formula for this is standard, and is given in many places.[30] The $\vec{k}$ dependence of the momentum matrix elements was included, as it is quite straightforward to evaluate the matrix elements using a basis of Gaussian orbitals. As in the calculation of the Compton profile, a grid of 506 points in $\frac{1}{48}$ of the zone was employed. A tetrahedral integra-

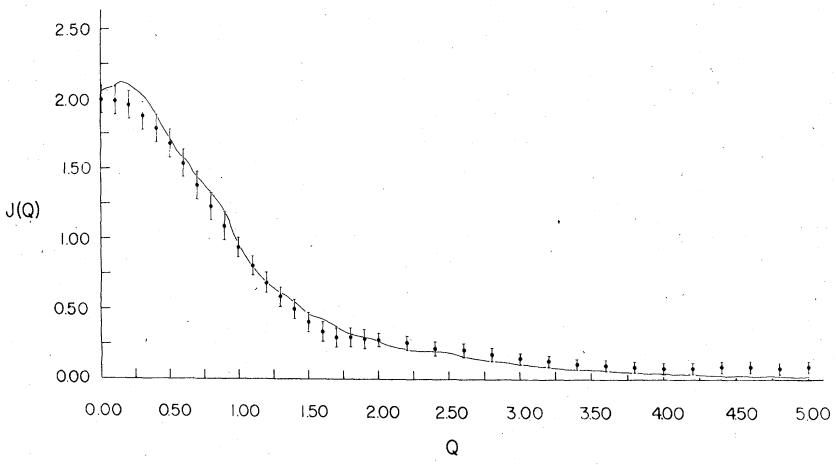

FIG. 6. Directionally averaged Compton profile. The experimental points are taken from Ref. 27.

tion method was used. The results are shown as the dashed curve in Fig. 8. Experimental measurements of Johnson and Christy[31] are also shown.

It is apparent that the measurements do not show the sharp structure of the calculated curve. A broad maximum occurs at about 2.8 eV, whereas the calculated conductivity has a maximum at 3.25 eV. There is an indication of a dip in the observed conductivity near 3.5 eV which may correspond to the calculated minimum at 3.75 eV. Finally, the experiments show a gentle rise beginning around 5.2 eV, which may relate to the computed maximum near 6.25 eV. The calculations show that many transitions in the zone contribute to both the 2.8 and 6.25 eV structure, but regions near the Σ

TABLE IV. Calculated Compton profile function in the [100], [110], and [111] directions together with the directional average profile.

q	$J_{[100]}$	$J_{[110]}$	$J_{[111]}$	J_{av}	q	$J_{[100]}$	$J_{[110]}$	$J_{[111]}$	J_{av}
0.0	1.765	2.139	2.255	2.062	2.6	0.180	0.158	0.145	0.161
0.1	1.832	2.162	2.260	2.093	2.7	0.145	0.144	0.141	0.144
0.2	2.006	2.139	2.171	2.109	2.8	0.124	0.128	0.127	0.126
0.3	2.077	2.012	1.987	2.025	2.9	0.113	0.114	0.133	0.119
0.4	1.950	1.870	1.853	1.889	3.0	0.105	0.100	0.110	0.104
0.5	1.798	1.692	1.662	1.714	3.1	0.086	0.092	0.099	0.092
0.6	1.678	1.552	1.517	1.579	3.2	0.064	0.087	0.090	0.081
0.7	1.588	1.370	1.395	1.439	3.3	0.058	0.078	0.081	0.073
0.8	1.491	1.234	1.309	1.327	3.4	0.065	0.069	0.072	0.069
0.9	1.214	1.148	1.240	1.190	3.5	0.076	0.065	0.057	0.066
1.0	0.850	1.042	0.963	0.967	3.6	0.075	0.059	0.051	0.061
1.1	0.668	0.907	0.783	0.807	3.7	0.061	0.053	0.048	0.054
1.2	0.625	0.765	0.624	0.689	3.8	0.051	0.048	0.046	0.048
1.3	0.673	0.629	0.541	0.619	3.9	0.045	0.045	0.046	0.045
1.4	0.657	0.509	0.502	0.550	4.0	0.042	0.042	0.042	0.042
1.5	0.535	0.434	0.435	0.463	4.1	0.039	0.038	0.041	0.039
1.6	0.429	0.395	0.469	0.424	4.2	0.032	0.035	0.039	0.035
1.7	0.362	0.361	0.402	0.372	4.3	0.024	0.032	0.034	0.030
1.8	0.327	0.304	0.349	0.322	4.4	0.022	0.029	0.031	0.028
1.9	0.305	0.280	0.317	0.297	4.5	0.024	0.027	0.028	0.026
2.0	0.253	0.264	0.289	0.267	4.6	0.028	0.024	0.024	0.025
2.1	0.191	0.245	0.262	0.234	4.7	0.027	0.022	0.022	0.023
2.2	0.176	0.217	0.229	0.210	4.8	0.023	0.021	0.017	0.020
2.3	0.193	0.206	0.181	0.196	4.9	0.020	0.019	0.018	0.019
2.4	0.227	0.196	0.162	0.196	5.0	0.018	0.018	0.017	0.018
2.5	0.225	0.181	0.148	0.185					

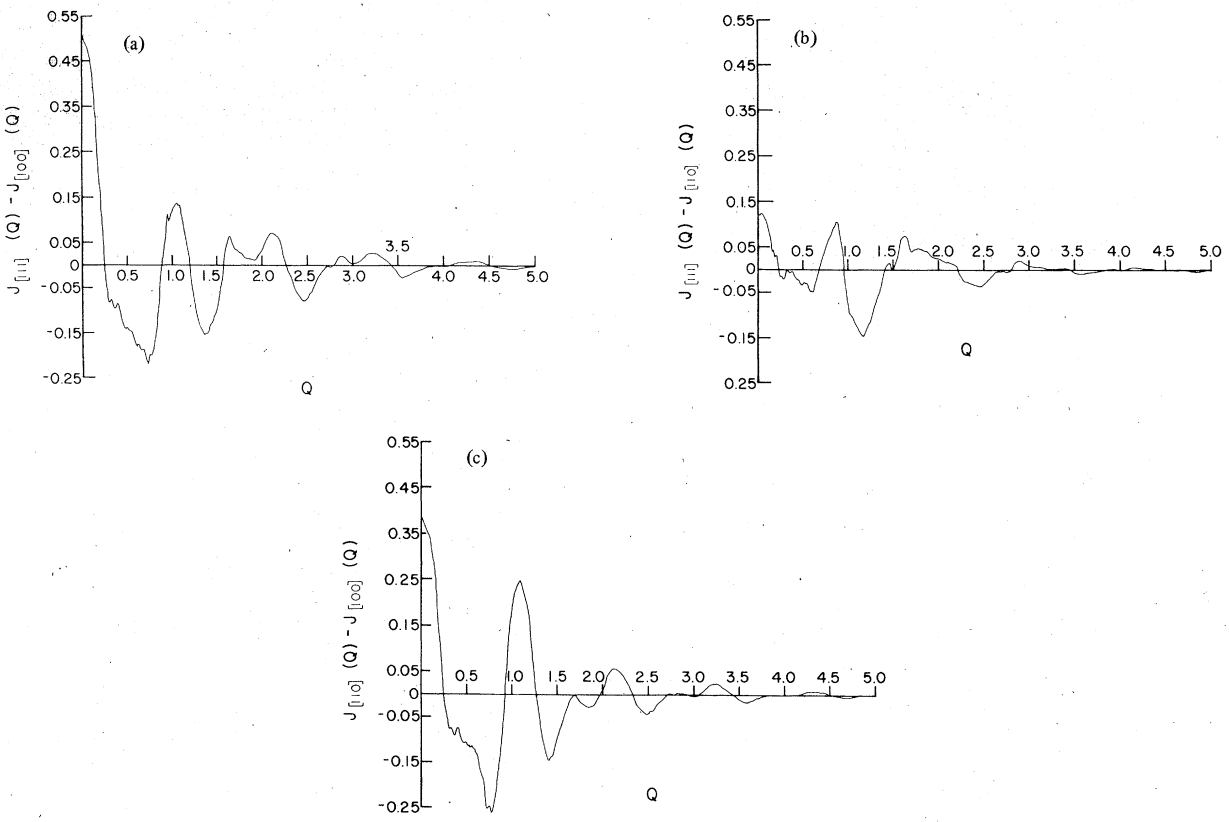

FIG. 7. (a), (b), (c) Anisotropy of the calculated Compton profile.

axis seem to be practicularly important in both cases.

We interpret the lack of sharp structure in the experimental data as probably indicating the presence of substantial lifetime broadening of the excited states. We have therefore investigated the effect of including a relaxation time in the conductivity calculation, as was done in our previous

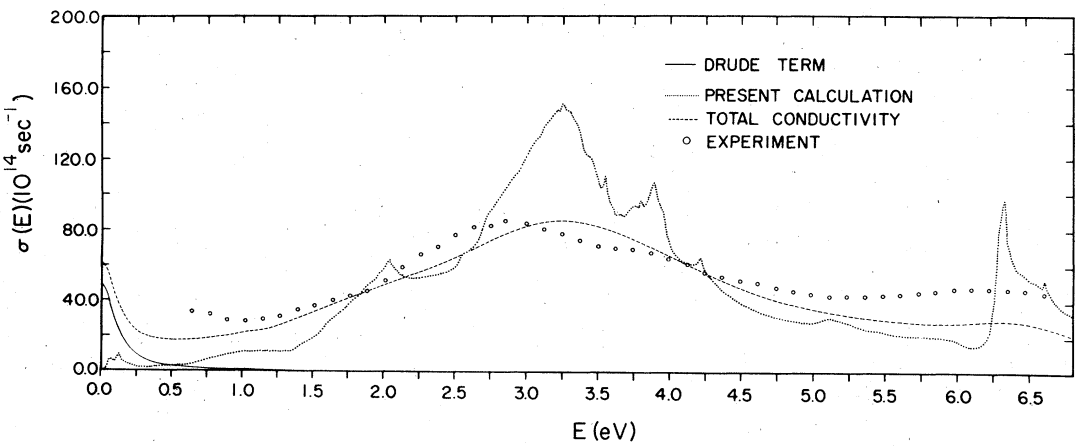

FIG. 8. Optical conductivity of vanadium. The dotted curve is the interband optical conductivity as calculated assuming the band states are sharp; the dashed curve includes a relaxation time $\hbar/\tau = 0.5$ eV. The solid curve is the Drude contribution. The experimental points are from Ref. 31.

study concerning nickel.[32] A reasonable degree of general agreement is obtained if $\hbar/\tau = 0.5$ eV. The results computed with this choice of τ are given as the solid curve in Fig. 8. In addition, we have added a Drude term at low energies, using parameters obtained from the long-wavelength measurements of Lenham and Treherne,[33] although the use of different relaxation times in this simple way may not be consistent with the sum rule for the conductivity. It is seen that the introduction of a relaxation time leads to a reasonable degree of general agreement between calculation and experiment. In a rough way, $\hbar/\tau \sim 0.5$ eV seems to be an optimum value. If 0.3 eV is used, the central peak is sharper than observed; for 0.7 eV, the smoothing is too great.

VI. CONCLUSIONS

The Kohn-Sham-Gasper exchange potential leads to an energy band structure in moderate agreement with experiment. The general structure of the Fermi surface is given correctly, although the specific cross-sectional areas are, with one exception, somewhat too large. The density of states is a major problem: one does not usually expect discrepancies of a factor of 2 in comparing band theory with experiment. The Compton profile has been computed, and awaits suitable experiments. The x-ray form factor agrees with limited experimental results. The optical conductivity agrees decently with experiment only when rather large lifetime broadening is included.

---

*Supported in part by the NSF.

†Present address: Department of Physics, Northwestern University, Evanston, Ill.

[1]L. F. Mattheiss, Phys. Rev. B 1, 373 (1970).
[2]J. R. Anderson, J. W. McCaffrey, and D. Papaconstantopoulos, Solid State Commun. 7, 1493 (1969).
[3]M. Yasui, E. Hayashi, and M. Shimizu, J. Phys. Soc. Jpn. 29, 1446 (1970).
[4]D. Papaconstantopoulos, J. R. Anderson, and J. W. McCaffery, Phys. Rev. B 5, 1214 (1972).
[5]S. Wakoh and J. Yamashita, J. Phys. Soc. Jpn. 35, 1394 (1973).
[6]T. M. Hattox, J. B. Conklin, J. C. Slater, and S. B. Trickey, J. Phys. Chem. Solids 34, 1627 (1973).
[7]L. D. Boyer, D. Papaconstantopoulos, and B. M. Klein, Phys. Rev. B 15, 3685 (1977).
[8]C. S. Wang and J. Callaway, Phys. Rev. B 15, 298 (1977).
[9]R. Gaspar, Acta Phys. Acad. Sci. Hung. 3, 263 (1954); W. Kohn and L. J. Sham, Phys. Rev. 140, A1133 (1965).
[10]A. J. H. Wachters, J. Chem. Phys. 52, 1033 (1970).
[11]O. Jepsen and O. K. Andersen, Solid State Commun. 9, 1763 (1971).
[12]G. Lehman and M. Taut, Phys. Status Solidi B 54, 469 (1972).
[13]J. Rath and A. J. Freeman, Phys. Rev. B 11, 2109 (1975).
[14]S. P. Singhal, Phys. Rev. B 12, 564 (1975); 12, 6007 (1975).
[15]D. E. Eastman, Solid State Commun. 7, 1697 (1969).
[16]C. F. Hague and C. Bonnelle, in *Band Structure Spectroscopy of Metals and Alloys*, edited by D. J. Fabian and L. M. Watson (Academic, New York, 1973), p. 251.
[17]We take the value recommended by F. Heininger, E. Bucher, and J. Muller [Phys. Kondens. Mater. 5, 243 (1966)]; determined by P. H. Keesom and R. Radebaugh [Phys. Rev. Lett. 13, 685 (1964)].
[18]W. L. McMillan, Phys. Rev. 167, 331 (1968).
[19]J. Callaway and C. S. Wang, Phys. Rev. B 16, 2095 (1977).
[20]R. D. Parker and M. Halloran, Phys. Rev. B 9, 4130 (1974).
[21]R. A. Phillips, Phys. Lett. A 36, 361 (1971).
[22]O. Terasaki, Y. Uchida, and D. Watanabe, J. Phys. Soc. Jpn. 39, 1277 (1975).
[23]R. J. Weiss and J. J. DeMarco, Phys. Rev. 140, A1223 (1965).
[24]M. Diana and G. Mazzone, Philos. Mag. 32, 1227 (1975).
[25]J. Rath, C. S. Wang, R. A. Tawil, and J. Callaway, Phys. Rev. B 8, 5139 (1973).
[26]S. Wakoh, Y. Kubo, and J. Yamashita, J. Phys. Soc. Jpn. 40, 1043 (1976).
[27]W. C. Phillips, Phys. Rev. B 7, 1047 (1973).
[28]S. Manninen and T. Pakkari, Physica Fennica 9, 129 (1974).
[29]O. Terasaki, T. Fukumachi, S. Hoysoya, and D. Watanabe, Phys. Lett. A 43, 123 (1973).
[30]For example, see W. Y. Ching and J. Callaway, Phys. Rev. B 11, 1324 (1975).
[31]P. B. Johnson and R. W. Christy, Phys. Rev. 139, 5056 (1974).
[32]C. S. Wang and J. Callaway, Phys. Rev. B 9, 4897 (1974).
[33]A. P. Lenham and D. M. Treherne, in *Optical Properties of Metals and Alloys*, edited by F. Abeles (North-Holland, Amsterdam, 1966), p. 196.